Journal of the Australian Ceramic Society (2022) 58:831–839
https://doi.org/10.1007/s41779-022-00731-4

RESEARCH

Comparison of electrical properties of ZnO-Bi_2O_3-based ceramics prepared by conventional and spark plasma sintering (SPS) methods

Fatih Apaydın[1] · Ali Çelik[2] · Ferhat Kara[2] · Hüseyin Özkan Toplan[3]

Received: 21 January 2022 / Revised: 23 February 2022 / Accepted: 6 March 2022 / Published online: 28 March 2022

Abstract

ZnO-Bi_2O_3-metal oxide systems are successfully utilized as varistors due to their non-linear I-V behavior. The electrical properties of ZnO-based varistors strongly depends on grain boundary phase composition and microstructural features. In this study, ZnO-based varistors containing different amount of CuO (0–2 mol%) were sintered by conventional and spark plasma sintering (SPS) methods, which resulted different I-V characteristics. While the samples sintered by SPS method were observed to have smaller grain size, more homogenous microstructure and higher density, grain boundary thickness reduced due to removal of bismuth, which was the result of high vacuum environment during sintering step. Since the barrier thickness of SPSed samples decreased, a lower breakdown electrical field (E_b) value was recorded in comparison to conventionally sintered samples. It was also detected that E_b values of both conventional and SPS samples increased with increasing CuO content.

Keywords Varistor · Bi_2O_3 · Spark plasma sintering (SPS) · I-V properties

Introduction

Zinc oxide (ZnO) is one of the most important metal oxides used as an n-type semiconductor due to the reasons as availability, environmentally friendly, and low cost of raw materials [1]. ZnO-based varistors are used to protect electronic circuits against voltage fluctuations thanks to their non-linear current–voltage (I-V) behavior, which is defined as the change in resistivity of a material at different applied voltages. When critical voltage is exceeded, the varistor protects the circuit elements thanks to the reduction in its electrical resistivity which results the current passing on varistor preferentially [2–5]. The electrical characteristics of ZnO varistors are strongly dependent on the phases and the microstructural properties such as grain size, shape, and distribution. A remarkable difference between resistivity of grain boundaries and grains are obtained by the dispersion of the additive phases, segregate at the grain boundaries during sintering. This difference in resistivity value is influenced by size and uniformity of additive phase as well as processing conditions [6]. The microstructure of ZnO varistors consists of conductive ZnO grains as matrix and various metal oxides which act as insulating barrier surrounding ZnO grains. Therefore, three characteristic regions present in I-V curves of the ZnO varistors. At low voltages, the insulating barrier between the grains results in a very high and almost Ohmic resistivity, which is called as pre-breakdown or Ohmic region. At a certain voltage, the threshold or breakdown voltage, the system enters the breakdown region in which the current increases abruptly, and the dependence of current on voltage is described by the empirical relation:

✉ Fatih Apaydın
fatih.apaydin@bilecik.edu.tr

Ali Çelik
acelik@eskisehir.edu.tr

Ferhat Kara
fkara@eskisehir.edu.tr

Hüseyin Özkan Toplan
toplano@sakarya.edu.tr

[1] Department of Metallurgical and Materials, Faculty of Engineering, Engineering, Bilecik Şeyh Edebali University, Bilecik, Turkey

[2] Department of Materials Science and Engineering, Faculty of Engineering, Eskişehir Technical University, Eskişehir, Turkey

[3] Department of Metallurgical and Materials Engineering, Faculty of Engineering, Sakarya University, Sakarya, Turkey

$$I = k V\alpha, \quad (1)$$

where $\alpha = d [\log (I)] / d [\log (V)]$. High nonlinear coefficient, which means faster time-response and more effective protection to devices, is regarded as the most significant index in varistor applications [7]. This parameter is a measure of the element nonlinearity, which varies with different voltage values. At higher current densities, the voltage starts to increase again resulting in an upturn region of the I-V characteristic [2].

The stability of ZnO varistors can be increased by glass and metal oxide additions. There are various additives investigated in the literature such as Sb_2O_3, MnO, BaO, Cr_2O_3, and CuO. [8–13]. Bi_2O_3 is one of the most attractive materials for ZnO varistors since it facilitates sintering by reducing the sintering temperature, promoting grain growth, and stabilizing nonlinear current–voltage characteristic of the material [9, 14, 15]. Peiteado et al. [16] made a kinetic analysis of grain growth to describe the relationship between breakdown voltage-sintering variables of ZnO-based varistors. They found that the varistor breakdown voltage can be calculated from the average size of the zinc oxide grains for a certain range of sintering conditions. This provides the evolution of varistor microstructure in a gradual and controlled manner and the distribution of the electrical interphases remains stable [16]. Rubia et al. [14] reported uncontrolled Bi_2O_3 evaporation during sintering and this can heavily impair the electrical properties of the varistors. They expressed considerable loss of bismuth as a result of interaction with the sintering atmosphere. Although increase in the surface area of Bi_2O_3 resulted an improved oxidation resistance, it also caused to increase in Bi evaporation. Therefore, they emphasized in their studies that there should be an optimum area/volume ratio, which balances both effects. Xu et al. [9] studied the I-V properties of the ZnO-Bi_2O_3 based varistor systems, which were sintered in three different routes (open sintering, closed crucible, and within powder beds) at the sintering temperatures in the range of 1000–1200 °C. They observed that the microstructure and, therefore, the electrical properties of varistors highly effected by the sintering methods and temperatures [9]. Mansour et al. [6] investigated the microstructural and electrical properties of ZnO-based varistors containing different amount of CuO. It was stated that the non-linear coefficient (α) and density increased with increasing CuO content. Similarly, Apaydın et al. [8] examined the effects of CuO addition into ZnO and showed that higher the amount of CuO promoted the grain growth.

Nowadays, progresses in nanotechnology have resulted in reduction of the size of the electronic devices as well as varistors. Therefore, there is always a strong demand for ceramic varistors with a much finer microstructures [17]. Indeed, such a microstructure yields a larger number of grain boundaries per unit volume and hence allows the production of components with identical performances with a lower weight to volume ratio in contrast to those currently on the market [17]. In order to achieve this, spark plasma sintering (SPS), which enables improved densification at much lower temperatures in short sintering times by loading with electrical energy, is a potential technique. Macary et al. [18] sintered ZnO-Bi_2O_3 varistor system via SPS method at relatively low temperatures between 550–600 °C. They reported that Bi_2O_3 leads to reduction in metallic bismuth transformation in an unexpected manner, which facilitates sintering at much lower temperatures. Beynet et al. [17] manufactured Bi_2O_3 and $Zn_7Sb_2O_{12}$ doped ZnO varistors by SPS at a temperature less than 400 °C lower than that of conventional sintered samples. They reported that the SPS inhibited growth of ZnO grains and reduced the transformation of Bi_2O_3 to metallic Bi during sintering.

It is well-known in the literature that the CuO contribution to ZnO increases the average grain size, breakdown voltage, nonlinearity coefficient, and density, while decreasing the leakage current [6, 19]. However, the effects of CuO addition to the ZnO-Bi_2O_3 system have not been sufficiently clarified in the literature. In this study, the microstructural and electrical properties of ZnO-based varistors prepared in ZnO-Bi_2O_3-CuO system (99-x mol% ZnO, 1 mol% Bi_2O_3, x mol% CuO composition) were investigated. Moreover, two different sintering technique (conventional and SPS) were utilized for the densification of the compositions and their effects on microstructural and electrical properties of the ZnO-based varistors were investigated, comparatively.

Experimental procedure

The powder batches were prepared by precise weighing of ZnO, Bi_2O_3, and CuO powders (99.99% pure) with a four digit scale in proper amounts. While the amount of Bi_2O_3 was kept constant for all composition (1 mol%), the content of CuO was altered between 0–2 mol%. The compositions were homogenized in isopropyl alcohol medium by a planetary ball mill for 2 h at a rotational speed of 300 rpm. The slurries were then dried by a rotary evaporator. The powders were compacted under 300 MPa into discs with the diameter and height of 13 mm and 2 mm, respectively. In order to prevent evaporation of Bi_2O_3, the conventional sintering temperature was selected as 1000 °C, which is slightly lower than a typical sintering temperature of ZnO-based varistors (1100 °C or above) reported in literature. In case of SPS, the samples were sintered at 800 °C, slightly lower than that of conventinal sintering thanks to the contribution of electirical current and mechanical loading on densification. The volatilization of Bi_2O_3 deteriorates the grain boundaries, and the large grain size of ZnO reduces the grain boundary areas between electrodes, causing a low breakdown electric field

[15]. In addition, the literature [17] and [18] stated that the SPS method is generally performed at lower temperatures. For these reasons, conventional sintering was carried out at 1000 °C and SPS at 800 °C. For conventional sintering, the pellets were sintered at 1000 °C for 1, 2, and 3 h at a constant heating and cooling rates (10 °C/min) under atmospheric condiditons. In case of SPS, compositions were transferred to a cylindrical graphite die with an inner diameter of 20 mm and sintered between the Cu-Be rams of SPS furnace at 800 °C for 5, 10, and 15 min dwell time under the uniaxial load of 16 kN. The surfaces of inner wall of die, upper, and lower punches in contact with the powder were covered by graphite papers for isolation. After SPS, the surface of the samples was ground with suitable SiC grinding papers in order to remove the carbon diffusion layer.

The bulk densities of the sintered samples were determined by the Archimedes method. The phases present in sintered samples were identified by X-ray diffraction (XRD) method.The thermal behavior of the compositions during sintering was determined by an optical dilatometer. The analysis were performed with a heating rate of 10 °C/min under atmospheric conditions. The microstructures of the samples were investigated by a scanning electron microscope (SEM) in backscattered electron (BE) mode. The elementel analysis of the samples was performed by energy disperse X-ray spectroscopy (EDS) attached to this SEM. The average ZnO grain size was calculated from the SEM images of each sample by using the Clemex software.

In order to determine electrical properties of the sintered samples, top and bottom surfaces of the sintered pellets were covered by gold–palladium alloy with a sputtering device. The I-V measurements of the varistor samples were carried out with high voltage source. The nonlinear coefficient (α) of the samples was obtained by Eq. (2) as follows:

$$\propto = \frac{logJ_2 - logJ_1}{logE_2 - \log E_1} \tag{2}$$

where J_1 and J_2 are current densities and equal to 0.1 mA.cm^{-2} and 1 mA.cm^{-2}, respectively. E_1 and E_2 are the electrical fields corresponding to J_1 and J_2, respectively. The breakdown electrical field E_b is determined as the field at current density 0.1 mA.cm^{-2}.

Results and discussion

Densification and microstructural properties of samples

The change in density of the sintered samples as a function of CuO content is given in Fig. 1. The density of the samples sintered by the conventional method and SPS increased with

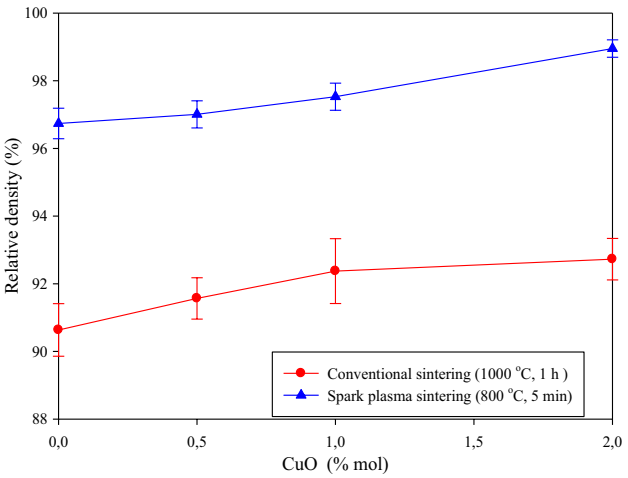

Fig. 1 The change in density of sintered samples as a function of CuO content

CuO content due to the reduction of eutectic temperature of the system, which is well agreed with [20]. The increase in densification of SnO_2-based varistors with CuO addition was also reported by Hu et al. [21]. Moreover, varistors produced by SPS method have been formed in a denser structure in comparison to the ones sintered by conventional method.

The thermal analysis curves of varistors containing different amounts of CuO are shown in Fig. 2. The first endothermic peak represents the eutectic point of the ZnO-Bi_2O_3 system, while the second peak, which becomes more prominent with the addition of 1% to 2% CuO, indicates the formation of Bi_2CuO_4 shown in Fig. 2a. The last peak indicates the formation of $Bi_{38}ZnO_{58}$. The thermal shrinkage curve in Fig. 2b shows the eutectic point of the ZnO-Bi_2O_3 system (numbered 1) decreases from 744 to 699 °C with the increase of CuO. In the same graph, it is seen that the formation temperatures of Bi_2CuO_4 and $Bi_{38}ZnO_{58}$ decrease with the increase of CuO content. Ikeda et al. [20] and Devisov et al. [22] found the same phase formations in their studies for similar varistor systems.

Figure 3a and b shows the back scattered electron (BE) SEM images and-EDX analysis taken from the points A, B, and C in corresponding image of 2% CuO doped ZnO sample sintered by conventional and SPS methods, respectively. While ZnO was observed as in gray color (1), the Bi-rich intergranular phase located around ZnO grains and triple pockets was seen as white regions (2). It is clear that the amount of Bi-rich intergranular phase in SPSed sample is much lower than that of conventionaly sintered samples. This is thought to be the result of high vacuum environment during SPS which causes evaporation of Bi_2O_3 from the system. According to the EDX results, Bi, Cu, and O elements were detected in the composition of the dark phase (3) rarely seen in the microstructure of conventianaly sintered samples.

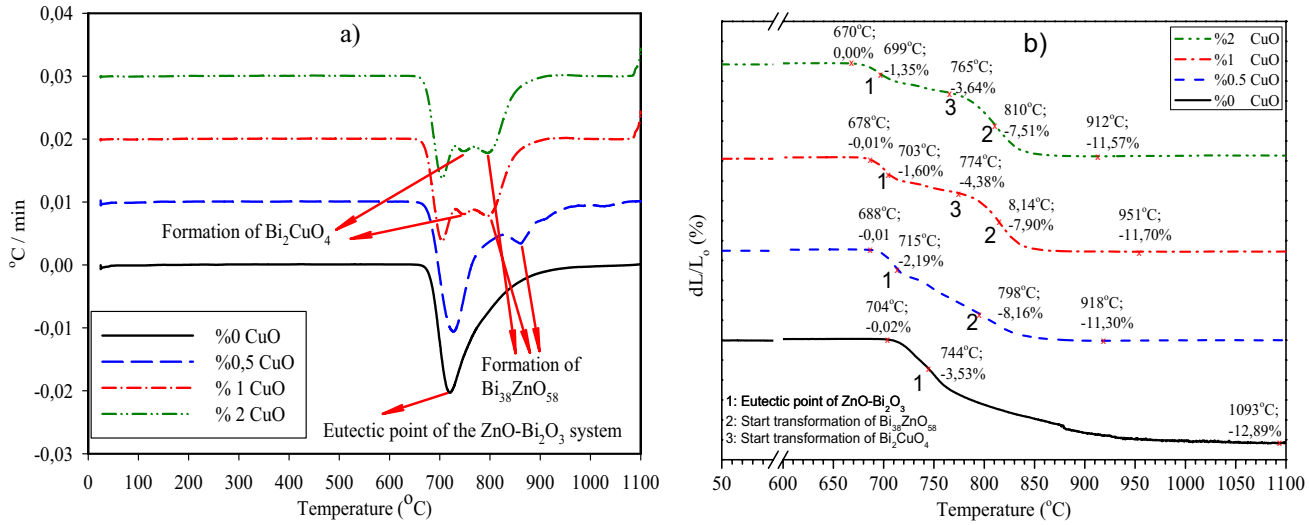

Fig. 2 Thermal analysis graphs of ZnO-Bi_2O_3-CuO varistors (**a** DTA, **b** Thermal shrinkage)

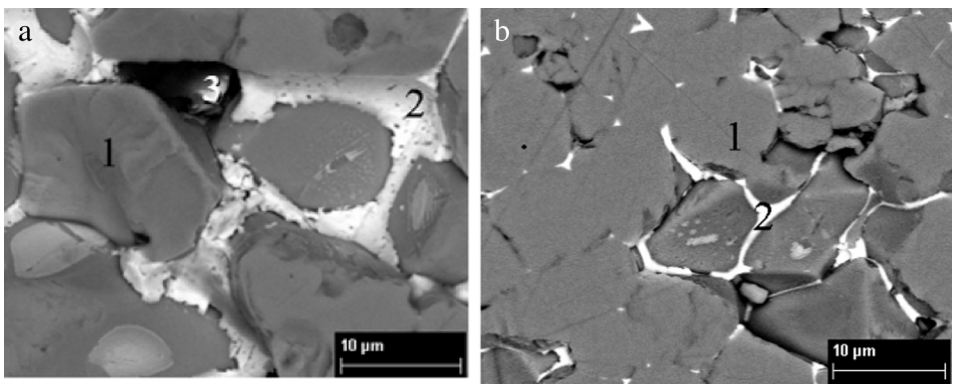

Fig. 3 SEM–EDS analysis of sintered samples. (**a** 1 h sintered by conventional method at 1000 °C, **b** sintered by SPS for 5 min at 800 °C)

	Zn (wt%)	Bi (wt%)	Cu (wt.%)	O
1	80.34	-	-	19.66
2	11.83	83.42	1.86	2.89
3	-	74.68	12.86	12.46

	Zn	Bi	Cu	O
1	80.78	-	-	19.22
2	34.34	59.42	2.20	4.05

On the other hand, this phase almost was not observed in the microstructure of SPSed sample (Fig. 3b).

XRD curves of varistors sintered with conventional method and SPS are shown in Fig. 4a and b. Figure 4a shows ZnO, Bi_2O_3, $Bi_{38}ZnO_{58}$, and Bi_2CuO_4 phases formed in varistors produced by conventional sintering. It is seen in Fig. 4b that ZnO, Bi_2O_3, and $Bi_{38}ZnO_{58}$ phases are formed in varistors sintered by SPS. The spinel formation was inhibited for SPSed samples due to the lack of Bi_2O_3 in the system. The formation of bismuth rich grain boundary phase as weel as spinel and pyrochars phases at triple pockets of conventionaly sintered ZnO-based varistors was also reported in [10, 18, 23]. In addition, De la Rubia et al. [24] and Straumal et al. [25] reported the formation of $Bi_{38}ZnO_{58}$ phase in ZnO-Bi_2O_3 phase systems.

SEM images of 0–2% CuO doped samples sintered by conventional and SPS methods are shown in Fig. 5. The increase in CuO content resulted to increase in grain size of both conventionally sintered and SPSed samples. It is clear in Fig. 5 that microstructures of the samples sintered via SPS method were much finer and homogeneous in comparison to the samples sintered by conventional method. This was attributed to the improved sintering mechanisms by the

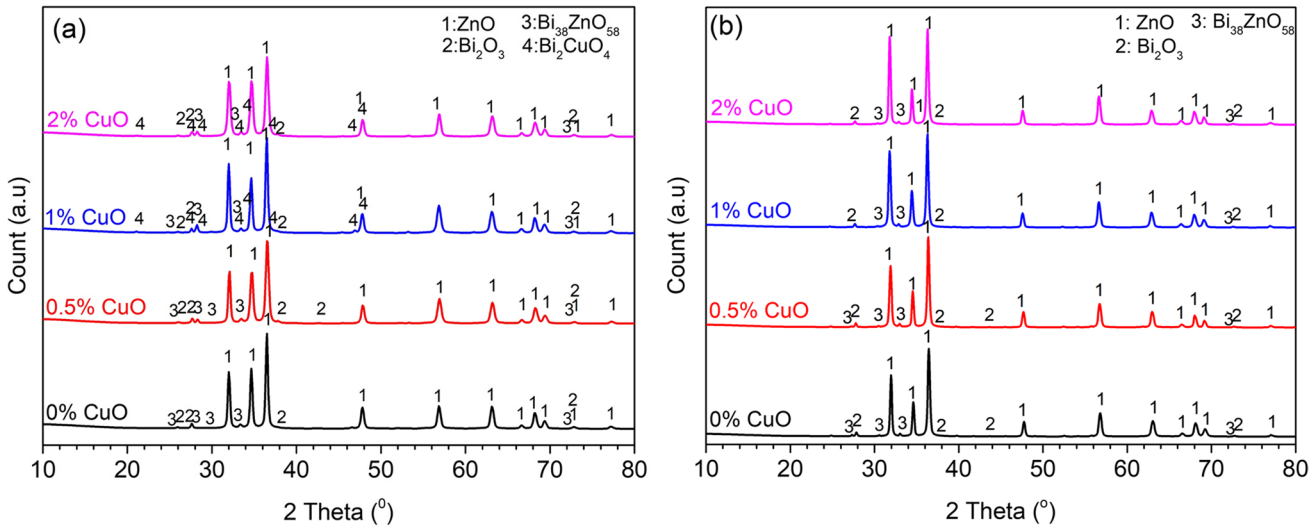

Fig. 4 XRD analysis of samples (**a** conventional sintered (0–0.5–1 and 2 CuO doped) varistors at 1000° C for 1 h, **b** SPS method sintered (0–0.5–1% and 2 CuO doped) varistors at 800° C for 5 min

effect of electrical current and mechanical pressure, which result efficient densification without any excessive grain growth. Another difference between the microstructures of the samples was the amount of Bi_2O_3-rich grain boundary phase. It was known that ZnO-Bi_2O_3 binary system has a eutectic reaction of ~ 738 °C [20], which is approximately 100 °C lower than sintering temperature utilized in this study. Moreover, the eutectic temperatures of the compositions were assumed to be lower than 738 °C in the presence of CuO, and, therefore, the evaporation became severe with increasing CuO content.

The change in grain size of the sintered samples were measured by linear intersection method on SEM images to compare grain growth of the samples sintered by two different techniques (Fig. 6 The grain size of the samples, sintered both conventional and SPS methods, increased with increasing CuO content. While the grain size of the conventionally sintered samples containing different amount of CuO increased parabolically, a slight and linear increment was observed for SPSed samples (Fig. 6). The increase in grain size was attributed to the reduction of eutectic temperature and the increase in liquid phase during sintering. This result is well agreed with [8]. The inhibition of the grain growth in SPSed samples was attributed to the much lower sintering temperature in limited dwell time.

Electrical characterization of the samples

The E-J curves of the sintered samples are shown in Fig. 7. The breakdown electrical field E_b is determined as the field at current density 0.1 mA.cm^{-2}. The nonlinear coefficient α was obtained by Eq. (1). The E-J curves of the conventionaly sintered samples (0–0.5–1% and 2 CuO doped) for 1 h at 1000 °C are shown in Fig. 7a. As the CuO content increased to 0–0.5–1 and 2%, the breakdown electrical field (E_b) increased by 121.2, 126.3, 199, 225.32 V/mm, respectively. This increase is attributed to higher thickness of the insulating barrier around the conductive ZnO boundaries in the presence of CuO. The E-J curves of the sintered samples (0–0.5–1% and 2 CuO doped) for 5 min at 800 °C by SPS method are shown in Fig. 7b. Similar to the conventionally sintered samples, the increase in CuO content increased the breakdown electrical field (E_b) values. As the CuO ratio increased to 0–0.5–1 and 2%, the breakdown electrical field (E_b) increased by 13.03, 19.81, 29.21, 77.61 V/mm, respectively. The E_b values for SPSed samples were much lower than that of conventionally sintered ones. This was assumed to be the result of severe evaporation of bismuth in the vacuum environment during SPS. The removal of bismuth from the system decreases the E_b value because it causes a decrease in the barrier in the ZnO varistor system [15]. Rubia et al. [14] stated that bismuth has a critical importance for the formation of electrically active grain boundaries and large amounts of evaporated Bi reduce the E_b value in the ZnO-Bi_2O_3 varistors system, because of which they produced in shapes with different area-to-volume ratios.

Figure 8a–c shows E_b and α curves of conventionally sintered at 1000 °C for 1, 2, and 3 h, respectively (calculated by the Eq. (1) in the range of 0.1–1 mA/mm^2). It was observed that E_b and nonlinear coefficient (α) of the samples increased with increasing CuO content but decreased with sintering time. Both max. E_b (225.32 V/mm) and max. α (34.5) values

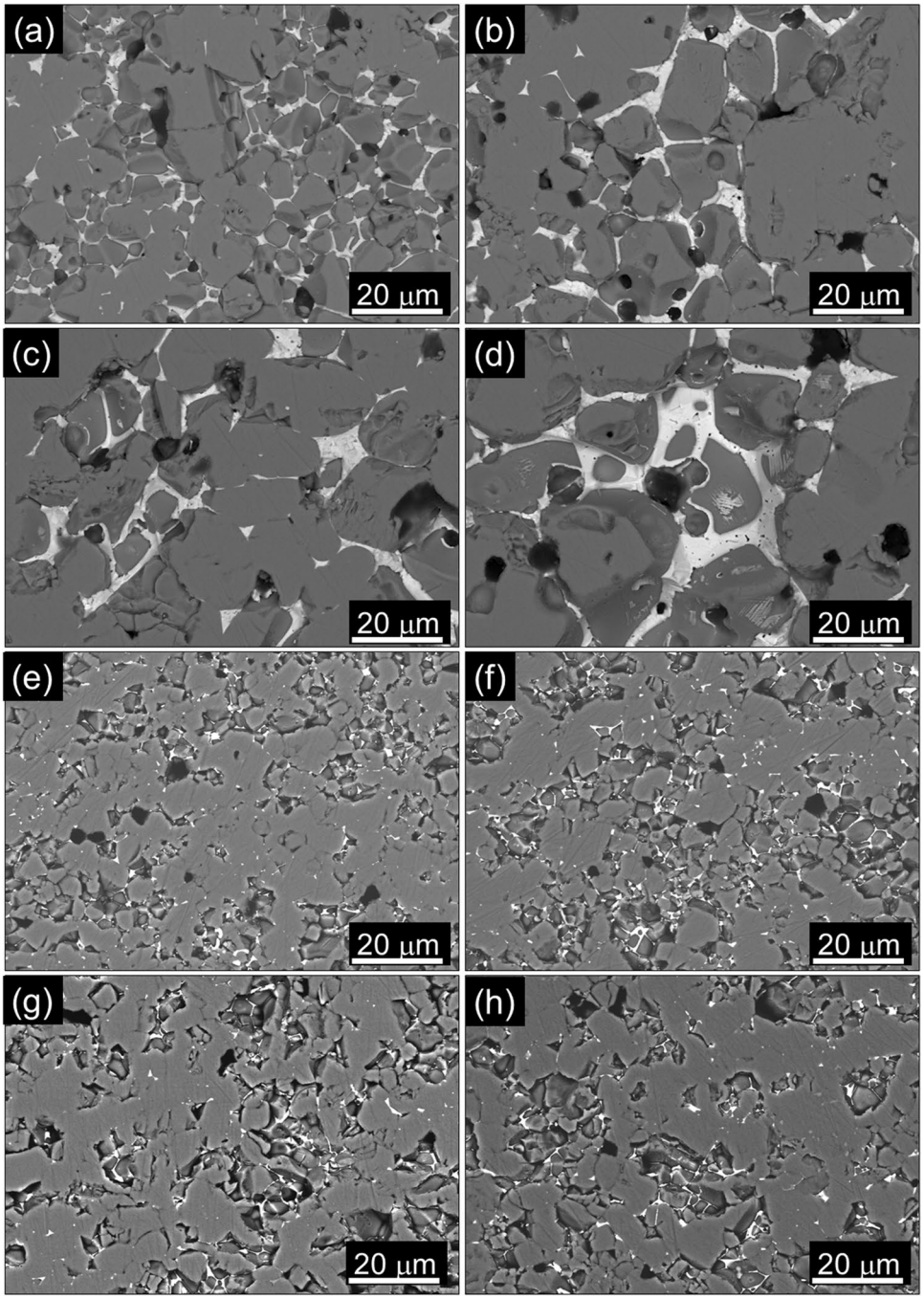

Fig. 5 SEM images of samples (**a** %0 CuO, **b** %0.5 CuO, **c** %1 CuO, **d** %2 CuO doped conventional sintering at 1000 °C for 1 h; **e** %0 CuO, **f** %0,5 CuO, **g** %1 CuO, **h** %2 CuO doped SPS method at 800 °C for 5 min)

were measured in the sintered for 1 h with 2% CuO added sample. The effects of CuO doping on (Co, Nb, Cr) doped SnO varistor were investigated by Hu et al. [21]. They stated that 0–0.2 mol% CuO additive reduces the leakage current value and adding more than 0.2% CuO increases the leakage current value. In addition, they reported the addition of CuO into the SnO_2 varistor, which decreased the E_b value. Similarly, Mansour et al. [26] added Cr_2O_3, Bi_2O_3, and NiO layers at different rates to the ZnO-CuO system and observed nonlinear coefficient (α) increased with the increase of CuO contribution in ZnO-based varistors.

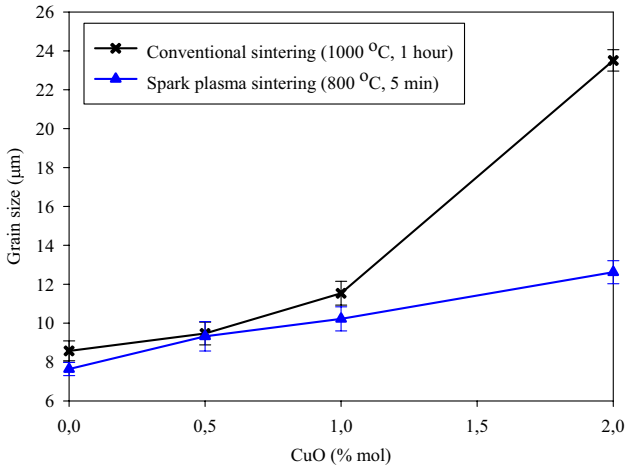

Fig. 6 % CuO-grain size relationship

Figure 8b–d shows E_b and α curves of samples sintered by SPS at 800 °C (calculated by the Eq. (1) in the range of 0.1–1 mA/mm^2). It was observed that E_b value increased with increasing CuO, but decreased with increasing sintering time. The maximum E_b (77.39 V/mm) value of the samples by SPS method was measured for 5 min sintering with 2% CuO addition. Besides, the maximum nonlinear coefficient (α) (17.6) value for the samples by SPS method was obtained from 5 min sintered sample with 1% CuO addition.

Conclusion

In this study, the microstructural and electrical properties of ZnO-Bi_2O_3-CuO (%99-x mol ZnO, 1% mol Bi_2O_3, %x mol CuO composition) based varistors prepared by conventional and spark plasma sintering (SPS) methods were compared. The following results were obtained:

- The samples produced by SPS method were observed to have smaller grain size, more homogenous microstructure, and higher bulk density. While the maximum relative density of 99.21% was obtained in the varistors sintered with SPS, the relative density of the varistors sintered conventionally was determined as 93.4% of theoretical density. With the addition of CuO into system from 0 to 2%, the grain size of the samples prepared by conventional sintering was measured as 8.47–23.55 µm. In case of SPS, the grain size was measured between 7.72 and 12.56 µm.
- It was observed that grain boundary thickness decreased in SPS due to bismuth removal resulted by vacuum during sintering. Since the barrier thickness of the samples produced by SPS method decreased, lower E_b values were obtained.
- The E_b value of both conventional and SPS samples increased with increasing CuO content. It has been measured that the E_b of varistors sintered with SPS is considerably lower than that of sintered conventionally because of the evaporation of Bi under vacuum conditions during SPS.

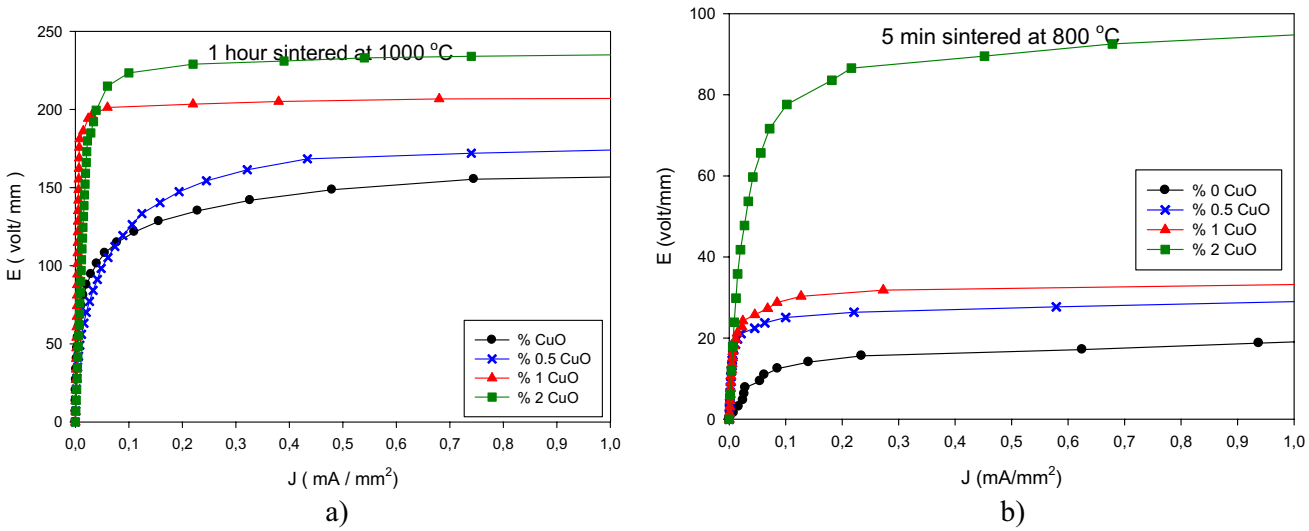

Fig. 7 E-J curves (**a** conventional sintering (1000 °C, 1 h), **b** SPS sintering (800 °C, 5 min)

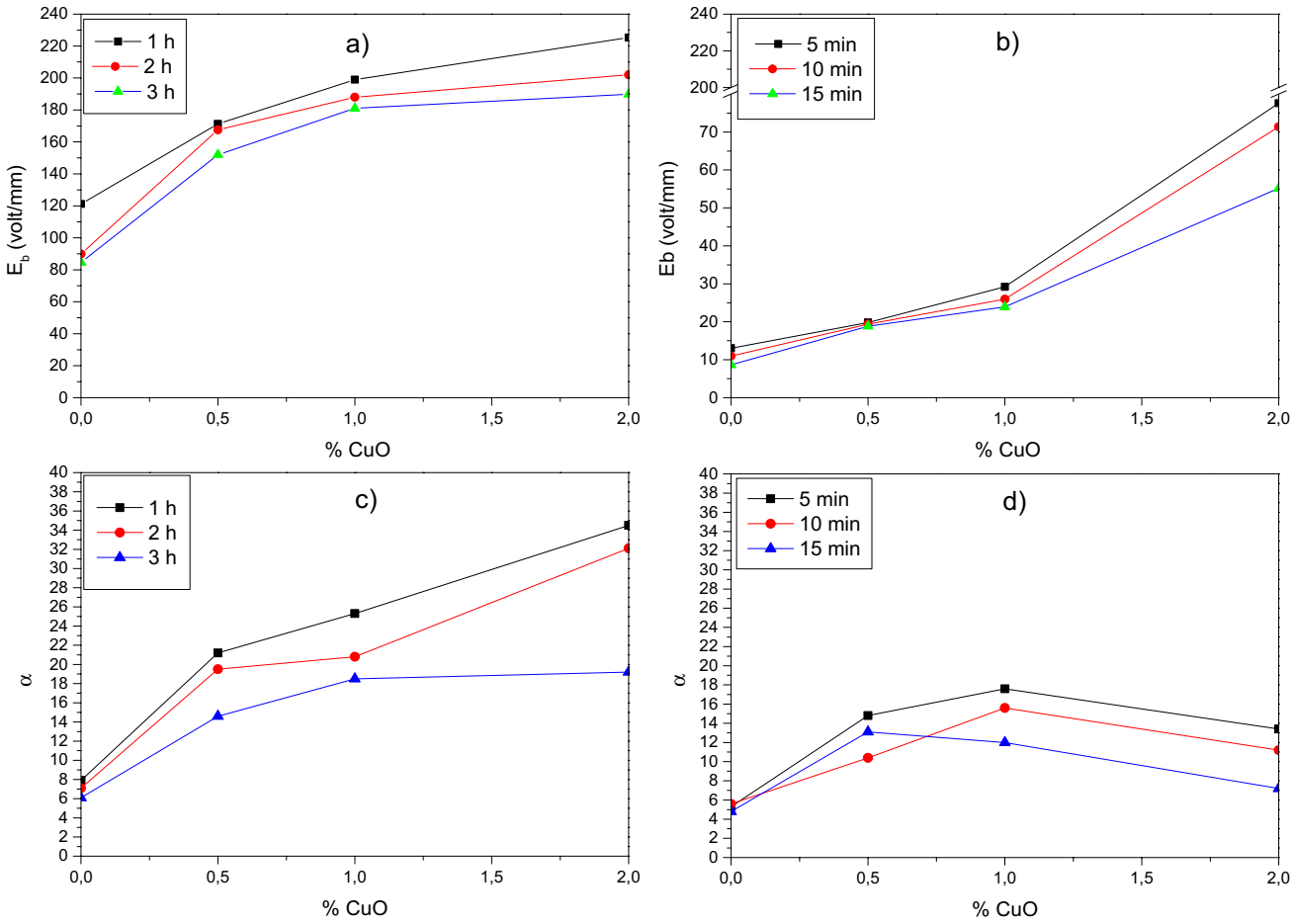

Fig. 8 Change in the E_b and α of varistors. (**a**, **c** sintered samples by conventional method at 1000 °C; **b**, **d** sintered samples by SPS method at 800 °C)

Author Contribution All listed authors contributed to the study. Fatih APAYDIN: Samples preparation, Data collection, and analysis, Writing-original draft. Ali ÇELİK: Microscopic characterization, Spark plasma sintering, Writing-review & editing, Ferhat KARA: Methodology, Supervision, Writing-review & editing, Özkan TOPLAN: Methodology, Supervision, Writing-review & editing. All authors read and approved the final manuscript.

Funding The study received financial support by Bilecik Şeyh Edebali University BAP coordinator under the project number 2016–02. BŞEÜ.03–04.

Declarations

Conflicts of interest The authors declare no competing interests.

References

1. Hopoğlu, H., Aydınoğlu, H.S., Özer, A., Tüzemen, E.Ş: Investigation of nitrogen doped ZnO thin films: effects on their structural and optical properties. Opt. Mater. **122**, 111685 (2021). https://doi.org/10.1016/j.optmat.2021.111685
2. Meshkatoddini, M. R.: Metal oxide ZnO-based varistor ceramics. Advances in ceramics-electric and magnetic ceramics, bioceramics, ceramics and environment. (2011)
3. Bokoro, P., Jandrell, I.: The impact of harmonics on the V− I characteristic of ZnO varistors. In 2016 IEEE International Conference on Dielectrics (ICD) (Vol. 2, pp. 658–661). IEEE. (2016)
4. Levinson, L.M., Philipp, H.R.: Zinc oxide varistors-a review. Am. Ceram. Soc. Bull. **65**(4), 639–646 (1986)
5. Kim, B., Seo, G.W., Ha, M., Hong, Y.W., Chung, C.Y.: Sintering process optimization of ZnO varistor materials by machine learning based metamodel. J. Korean Cryst. Growth Cryst. Technol. **31**(6), 258–263 (2021). https://doi.org/10.6111/JKCGCT.2021.31.6.258
6. Saadeldin, M.M., Desouky, O.A., Ibrahim, M., Khalil, G.E., Helali, M.Y.: Investigation of structural and electrical properties of ZnO varistor samples doped with different additives. NRIAG J. Astron. Geophys. **7**(2), 201–207 (2018). https://doi.org/10.1016/j.nrjag.2018.06.002
7. Bai, H., Li, M., Xu, Z., Chu, R., Hao, J., Li, H., Li, G.: Influence of SiO_2 on electrical properties of the highly nonlinear

ZnO-Bi_2O_3-MnO_2 varistors. J. Eur. Ceram. Soc. **37**(13), 3965–3971 (2017). https://doi.org/10.1016/j.jeurceramsoc.2017.05.014
8. Apaydin, F., Toplan, H.Ö., Yildiz, K.: The effect of CuO on the grain growth of ZnO. J. Mater. Sci. **40**(3), 677–682 (2005)
9. Xu, D., Shi, L., Wu, Z., Zhong, Q., Wu, X.: Microstructure and electrical properties of ZnO–Bi_2O_3-based varistor ceramics by different sintering processes. J. Eur. Ceram. Soc. **29**, 1789–1794 (2009). https://doi.org/10.1016/j.jeurceramsoc.2008.10.020
10. Senda, T., Bradt, R.C.: Grain Growth in sintered ZnO and ZnO-Bi_2O_3 ceramics. J. Am. Ceram. Soc. **73**(1), 106–114 (1990). https://doi.org/10.1111/j.1151-2916.1990.tb05099.x
11. Han, J., Mantas, P.Q., Senos, A.M.R.: Grain growth in Mn-doped ZnO. J. Eur. Ceram. Soc. **20**(16), 2753–2758 (2000). https://doi.org/10.1016/S0955-2219(00)00220-X
12. Fan, J., Freer, R.: Varistor properties and microstructure of ZnO–BaO ceramics. J. Mater. Sci. **32**(2), 415–419 (1997). https://doi.org/10.1023/A:1018561602083
13. Yongvanich, N., Visuttipitukkul, P., Parnem, R., Sittikeadsakun, A., Wittayaprasopchai, A.: Influence of chromium on microstructure and electrical properties of ZnO-based varistor materials. Energy Procedia **9**, 474–482 (2011). https://doi.org/10.1016/j.egypro.2011.09.054
14. De la Rubia, M.A., Peiteado, M., Fernandez, J.F., Caballero, A.C.: Compact shape as a relevant parameter for sintering ZnO–Bi_2O_3 based varistors. J. Eur. Ceram. Soc. **24**(6), 1209–1212 (2004). https://doi.org/10.1016/S0955-2219(03)00410-2
15. Zhao, X., Liang, J., Sun, J., Guo, J., Dursun, S., Wang, K., Randall, C.A.: Cold sintering ZnO based varistor ceramics with controlled grain growth to realize superior breakdown electric field. J. Eur. Ceram. Soc. **41**(1), 430–435 (2021). https://doi.org/10.1016/j.jeurceramsoc.2020.09.023
16. Peiteado, M., Fernández, J.F., Caballero, A.C.: Varistors based in the ZnO–Bi_2O_3 system: microstructure control and properties. J. Eur. Ceram. Soc. **27**(13–15), 3867–3872 (2007). https://doi.org/10.1016/j.jeurceramsoc.2007.02.046
17. Beynet, Y., Izoulet, A., Guillemet-Fritsch, S., Chevallier, G., Bley, V., Pérel, T., Estournès, C.: ZnO-based varistors prepared by spark plasma sintering. J. Eur. Ceram. Soc. **35**(4), 1199–1208 (2015). https://doi.org/10.1016/j.jeurceramsoc.2014.10.007
18. Saint Macary, L., Kahn, M., Estournès, C., Fau, P., Trémouilles, D., Bafleur, M., Chaudret, B.: Size effects on varistor properties made from zinc oxide nanoparticles by low temperature spark plasma sintering. Adv. Funct. Mater. 19(11), 1775 (2009). https://hal.archives-ouvertes.fr/hal-00383348
19. Bellini, J.V., Morelli, M.R., Kiminami, R.H.: Ceramic system based on ZnO CuO obtained by freeze-drying. Mater. Lett. **57**(24–25), 3775–3778 (2003). https://doi.org/10.1016/S0167-577X(03)00177-0
20. Ikeda, Y., Sano, Y., Bando, Y., Niinae, T., Takada, J.: Consideration of Bi_2CuO_4 in the Bi_2O_3-CuO system. J. Jpn. Soc. Powder Powder Metall. **41**(4), 384–387 (1994). https://doi.org/10.2497/jjspm.41.384
21. Hu, G., Zhu, J., Yang, H., Wang, F.: Effect of CuO addition on the microstructure and electrical properties of SnO_2-based varistor. J. Mater. Sci.: Mater. Electron. **24**(8), 2944–2949 (2013). https://doi.org/10.1007/s10854-013-1195-1
22. Denisov, V.M., Irtyugo, L.A., Denisova, L.T., Kirik, S.D., Chumilina, L.G.: High-temperature heat capacity of Bi_2CuO_4. Phys. Solid State **54**(9), 1943–1945 (2012). https://doi.org/10.1134/S1063783412090089
23. Kuo, S.T., Tuan, W.H., Lao, Y.W., Wen, C.K., Chen, H.R.: Grain growth behavior of Bi_2O_3-doped ZnO grains in a multilayer varistor. J. Am. Ceram. Soc. **91**(5), 1572–1579 (2008). https://doi.org/10.1111/j.1551-2916.2008.02309.x
24. De la Rubia, M.A., Fernandez, J.F., Caballero, A.C.: Equilibrium phases in the Bi_2O_3-rich region of the ZnO–Bi_2O_3 system. J. Eur. Ceram. Soc. **25**(12), 2215–2217 (2005). https://doi.org/10.1016/j.jeurceramsoc.2005.03.033
25. Straumal, B., Mazilkin, A., Straumal, P., Myatiev, A.: Distribution of impurities and minor components in nanostructured conducting oxides. Int. J. Nanomanuf. **2**(3), 253–270 (2008)
26. Mansour, S.E., Desouky, O.A., Negim, S.M., Kamil, W.A.: Microstructure and Current-voltage Characteristics of (ZnO-CuO) Varistor System in the Presence of Additive Oxides, Cr_2O_3, Bi_2O_3 and NiO. Curr. Res. Chem. **3**, 29–48 (2011). https://doi.org/10.3923/crc.2011.29.48